

See discussions, stats, and author profiles for this publication at: <https://www.researchgate.net/publication/263942490>

# Raman Staircase in Charge Transfer SERS at the Junction of Fusing Nanospheres

ARTICLE *in* JOURNAL OF PHYSICAL CHEMISTRY LETTERS · DECEMBER 2012

Impact Factor: 7.46 · DOI: 10.1021/jz3018072

CITATIONS

9

READS

30

## 4 AUTHORS:



[Mayukh Banik](#)

University of California, Irvine

10 PUBLICATIONS 72 CITATIONS

[SEE PROFILE](#)



[Vartkess Ara Apkarian](#)

University of California, Irvine

193 PUBLICATIONS 4,047 CITATIONS

[SEE PROFILE](#)



[Tae-Ho Park](#)

Colorado School of Mines

28 PUBLICATIONS 535 CITATIONS

[SEE PROFILE](#)



[Michael Galperin](#)

University of California, San Diego

82 PUBLICATIONS 2,472 CITATIONS

[SEE PROFILE](#)

# Raman Staircase in Charge Transfer SERS at the Junction of Fusing Nanospheres

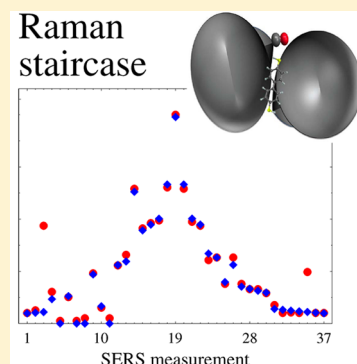
M. Banik,<sup>†</sup> V. A. Apkarian,<sup>\*,†</sup> T.-H. Park,<sup>‡</sup> and M. Galperin<sup>\*,‡</sup>

<sup>†</sup>Department of Chemistry, University of California, Irvine, California 92697, United States

<sup>‡</sup>Department of Chemistry and Biochemistry, University of California, San Diego, California 92093, United States

## Supporting Information

**ABSTRACT:** We present a theoretical analysis of Raman intensities for a molecule that bridges a current carrying junction. Experimental data is used to estimate parameters for the theoretical model. The recently reported staircase of Raman intensities observed during the fusion of nanodumbbell is reproduced.



**SECTION:** Physical Processes in Nanomaterials and Nanostructures

Surface enhanced Raman spectroscopy (SERS) of molecules was originally recognized for pyridine chemisorbed on silver electrodes.<sup>1</sup> There have been extensive developments of the field since then, both in experimental and theoretical fronts.<sup>2</sup> Early on, the observation of SERS was explained by a combination of surface plasmon resonance of the metal<sup>3</sup> and charge transfer (CT) between molecule and metal.<sup>4</sup> Plasmon excitations caused by incident light produce large local electric fields (“hot spots”) making observation of a weak molecular optical response feasible. Advances in experimental techniques have enabled the recording of SERS of single molecules attached to single nanoparticles.<sup>5</sup> More recently, the ability to form nanoscale gaps supporting “hot spots”<sup>6,7</sup> ushered a new field of research aimed at interrogating single molecule conduction junctions with light.<sup>8</sup> Such measurements have the potential of becoming a diagnostic and control tool in molecular electronics.

In single molecule SERS experiments, the Raman signal fluctuates<sup>5,19</sup> due to the instability of either the nanoparticles, the molecule, or coupling between the two. Relying on the synthetic strategy to link nanospheres through a dithiolate,<sup>20</sup> it has been possible to scrutinize SERS fluctuations of a molecule immobilized at the plasmonic hot spot of the junction.<sup>21</sup> Taking advantage of the tensorial nature of SERS, detailed mechanistic assignment has been derived from the observed SERS trajectories.<sup>22</sup> In particular, it was noted that, in the conductivity limit of the plasmon,<sup>23–27</sup> the scattering intensity grows exponentially as the gap closes. Moreover, in the case of CO chemisorbed at the junction, a staircase structure is seen in intensity as the gap closes and reopens. The latter observation

inspires the consideration of a model where the junction current is quantized due to atom–atom contacts made sequentially during the dumbbell fusion process. While quantization of transport in molecular junctions is well-known, and quanta of electrical<sup>28</sup> and thermal<sup>29</sup> conductance were reported in the literature, the observation of a staircase in the Raman scattering intensity is a new feature.

The experiments are joint atomic force microscopy (AFM) and Raman spectroscopy conducted on individual nanodumbbells, consisting of silver nanospheres (30 nm) linked through

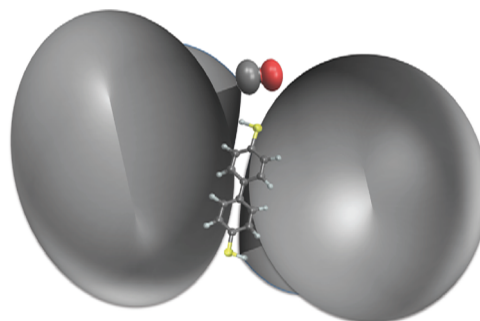


**Figure 1.** A schematic of the dumbbell. It consists of two silver spheres (~ 30 nm) chemically linked by DBDT. The CO molecule is chemisorbed on an asperity at the hot spot of the junction.

**Received:** November 6, 2012

**Accepted:** December 11, 2012

dibenzyl-dithiol (DBDT; see schematic in Figure 1). The spectrum of the DBDT is used to characterize the local fields and field-molecule orientation. The data set of interest here is a SERS trajectory sequence in which a CO molecule appears at the intersphere hot spot. Owing to its linear Stark shift, the CO spectrum serves as a quantitative gauge of the local field. During the sequence, recorded at a speed of 10 s/spectrum, the local field measured by the spectral shift of CO increases linearly from 0 to 1.2 V/Å (see Figure 2a). Moreover, due to poor

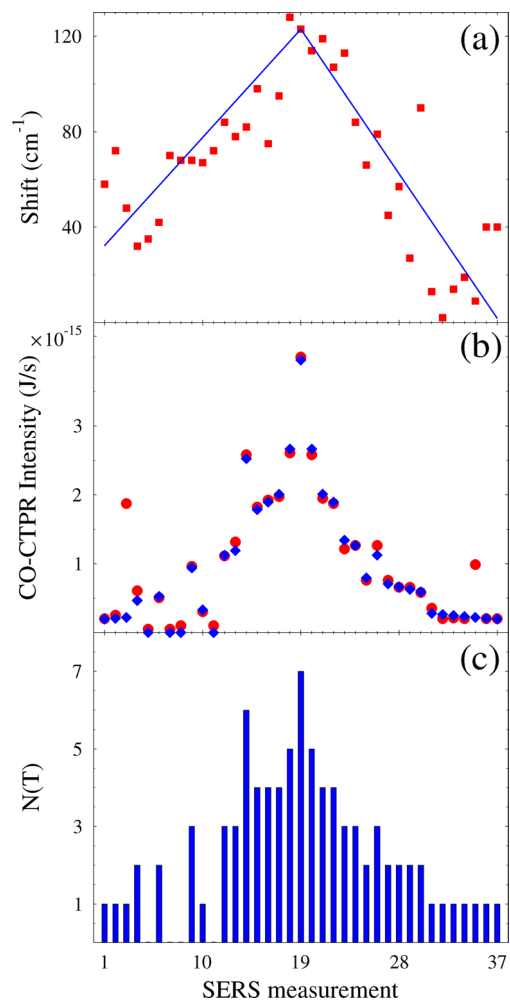


**Figure 2.** Calculation of the intensity of the CO-CTPR band for a sequence of the recorded SERS spectra. Experimental data from ref 18 are compared to results of simulation. Shown are (a) fit of the Stark shift  $\Delta\omega_v$  (lines, blue) to experimental data (squares, red), (b) comparison between measured (circles, red) and calculated (diamonds, blue) (eq 7) Stokes intensities of the CO-CTPR signal and (c) the number of scattering channels  $N(T)$  for different spectra  $T$ .

chemisorption energy of CO on noble metals, its presence at the junction establishes that it is bonded atop an atomically sharp protrusion, and that the junction temperature does not exceed 350 K. The experimental data yield a sequence of intensities of the CO line assigned to the charge transfer plasmon resonance (CTPR). Intensity of the experimental signal is estimated according to  $I = \eta f I_0 \sigma$ , where  $\eta \sim 0.01$  is an efficiency factor,  $f = 10^{12}$  is the enhancement factor,  $I_0 = 1 \text{ mW}/\mu\text{m}^2$  is the typical laser intensity, and  $\sigma = 4 \times 10^{-30} \text{ cm}^2$  is the absolute scattering cross section of CO. The AFM images taken

before and after recording the SERS trajectories show that a neck has developed between the spheres, indicative of fusion accompanied by the transfer of silver atoms.

Here we discuss theoretically a mechanism for the observed staircase in the CO CTPR. Experimental evidence of silver atom transfer suggests the formation (and destruction) of metallic bridges between the two nanoparticles during their fusion. Such bridges, assumed to be independent channels for conductance, yield quantized contributions to the CT Raman scattering intensity caused by tunneling electrons interacting with the CO vibration. Note that metallic bridge formation also affects local electromagnetic field formation, which yields changes in vibrational Stark shift. However, the shift is defined by the chemical potential determined by the overall asymmetry of the junction. It evolves continuously as the gap closes, and is not expected to be quantized (see, e.g., ref. 30 for recent discussion). Indeed, the linear fit to the shift (see Figure 2a) is used as a calibration of the continuous gap distance. We will conclude that quantization of the current is the mechanism for the observed Raman staircase.

Theoretically, a comprehensive description of Raman spectroscopy in molecular junctions is a challenging problem on the interface of classical and quantum theories,<sup>9</sup> which involves coupled plasmon and molecular dynamics. The former is usually described within laws of classical electrodynamics, and the latter relies on nonequilibrium quantum statistical mechanics.<sup>10–13</sup> Another important ingredient of the problem is the ability to describe light (Raman) scattering in molecular current-carrying junctions. The requisite theory at a model level was developed in a number of our recent publications.<sup>14–17</sup> We apply this formalism to model observations made in a recent SERS study on a fusing nanojunction.<sup>18</sup> Previously we have discussed the correlation between electric current and CT Raman spectroscopy in a model of single tunneling channel.<sup>31,32</sup> Here we extend this consideration to demonstrate that indeed a staircase is to be expected at a junction where atomic contacts are made. The theoretical model stands on its own. However, we use parameters deduced from the experimental data and show that the model is fully consistent with the observations reported in ref 18.

We distinguish two time scales in the problem. The first ( $t$ ) characterizes electron transport in the junction and photon scattering events. It is assumed to be fast relative to the second time scale ( $T$ ), related to the slow motion ( $\sim 1 \text{ Å/min}$ ) of the nanoparticles. By the usual time scale separation argument, we perform fully quantum mechanical consideration of Raman scattering in a molecular junction, keeping  $T$  as a parameter. (Note: Below we use  $T$  to number the spectra.) The junction consists of the two nanoparticles,  $L$  and  $R$ , connected by a number of independent scattering channels,  $N(T)$ , with energies  $\varepsilon_n$  and a molecule characterized by vibrational frequency  $\omega_v$ . The nanoparticles are excited by the external field  $\vec{E}(t) = \vec{E}_0 \cos(\nu t)$ . This field is assumed to be strong enough to justify its classical consideration.

The Hamiltonian of the system is (here and below  $\hbar = 1$ )

$$\hat{H}(T, t) = \hat{H}_0(T, t) + \hat{V}(T) \quad (1)$$

$$\begin{aligned} \hat{H}_0(T, t) = & \sum_{n=1}^{N(T)} \varepsilon_n \hat{a}_n^\dagger \hat{a}_n + \omega_v(T) \hat{v}^\dagger \hat{v} + \sum_{k \in L, R} \varepsilon_k(t) \hat{c}_k^\dagger \hat{c}_k \\ & + \sum_f \nu_f \hat{a}_f^\dagger \hat{a}_f \end{aligned} \quad (2)$$

$$\hat{V}(T) = \sum_{n=1}^{N(T)} [M_v(\hat{v} + \hat{v}^\dagger)\hat{d}_n^\dagger\hat{d}_n + \sum_{k \in L,R} (V_{kn}(T)\hat{c}_k^\dagger\hat{d}_n + H. c.) + \sum_f U_f(\hat{a}_f + \hat{a}_f^\dagger)\hat{d}_n^\dagger\hat{d}_n] \quad (3)$$

where  $\hat{d}_n^\dagger$  ( $\hat{d}_n$ ) and  $\hat{c}_k^\dagger$  ( $\hat{c}_k$ ) are creation (annihilation) operators for electrons in the electronic tunneling channel  $n$  and in the state  $k$  of the contacts, and  $\hat{v}^\dagger$  ( $\hat{v}$ ) and  $\hat{a}_f^\dagger$  ( $\hat{a}_f$ ) create (destroy) quantum of molecular vibration and photon in the mode  $f$ , respectively. External driving in the contacts is assumed to be harmonic  $\varepsilon_k(t) = \varepsilon_k^0 + A_K \cos(\nu_i t)$ , where  $A_K = \pm (\vec{\mu} \cdot \vec{E}_0)$  with  $+$  ( $-$ ) corresponding to  $K = L$  ( $R$ ). Note that the classical field  $\vec{E}(t)$  and quantum operators  $\hat{a}_f^\dagger$  ( $\hat{a}_f$ ) represent different modes of the same radiation field. It is customary to consider a “pumping mode” separately from the rest of the field modes (“accepting modes”).<sup>33,34</sup> The latter serve as an optical detector for photon flux coming out of the system.

Equations 1–3 are a variant of a model for the CT contribution to SERS originally proposed in ref 35 for an

equilibrium system describing a molecule attached to a metal surface, and extended to nonequilibrium steady-state situation in our recent publication.<sup>36</sup> The time-dependent version of the model was discussed in refs 31 and 32. Here we generalize the latter consideration to the multilevel model with external driving in the contacts, which is more relevant for the present case.

Following the steps that lead to derivation of eq 40 of ref 32 and utilizing analytical results for harmonic driving in contacts,<sup>37</sup> we get for the particle Raman flux (see Supporting Information)

$$J_{i \rightarrow f}(t) = 2|U_f|^2|M_v|^2 \sum_{n=1}^{N(T)} \text{Re} \int_{-\infty}^t dt' e^{i\nu_f(t-t')} \times (N_v P_n^r(T; t, \omega_v(T)) P_n^a(T; \omega_v(T), t') + [1 + N_v] P_n^r(T; t, -\omega_v(T)) \times P_n^a(T; -\omega_v(T), t')) \quad (4)$$

where  $N_v$  is the thermal population of the molecular vibration,

$$P_n^r(T; t, \omega) \equiv -i \sum_{K=L,R} \sum_{m_1, m_2=-\infty}^{+\infty} J_{m_1}\left(\frac{A_K}{\nu_i}\right) J_{m_2}\left(\frac{A_K}{\nu_i}\right) \times e^{-i[\omega + (m_2 - m_1)\nu_i]t} \int_{-\infty}^{+\infty} \frac{dE}{2\pi} \Sigma_{K,n}^<(T; E) \{1/[(E - \varepsilon_n + m_2\nu_i + i\Gamma_n(T)/2)(E - \varepsilon_n + m_1\nu_i - i\Gamma_n(T)/2)]\} \times \left( \frac{1}{E + \omega - \varepsilon_n + m_2\nu_i + i\Gamma_n(T)/2} + \frac{1}{E - \omega - \varepsilon_n + m_1\nu_i - i\Gamma_n(T)/2} \right) \quad (5)$$

and  $P_n^a(T; \omega, t') \equiv [P_n^r(T; t', \omega)]^*$ . In eq 5  $J_m(\dots)$  is the Bessel function,  $\Gamma_n(T; E) \equiv \Sigma_{K=L,R} \Gamma_n^K(T; E) = 2\pi \Sigma_{K=L,R} |V_{kn}(T)|^2 \delta(E - \varepsilon_k^0)$  is the total electron escape rate (in the wide-band approximation assumed here,  $\Gamma_n^K$  does not depend on energy  $E$ <sup>38</sup>), and  $\Sigma_{K,n}^<(T; E)$  is the lesser self-energy due to coupling of the resonance  $n$  to the contact  $K$  ( $= L, R$ )

$$\Sigma_{K,n}^<(T; E) \equiv i\Gamma_n^K(T) f_K(E) \quad (6)$$

where  $f_K(E)$  is the Fermi distribution in the contact  $K$  in the absence of the driving field.

Corresponding Raman intensity is (intensity is defined as an energy flux averaged over the period of oscillation)

$$I = \int d\nu_i \int d\nu_f \rho(\nu_i) \rho(\nu_f) \nu_f \langle J_{i \rightarrow f}(t) \rangle \quad (7)$$

where  $\rho(\nu) \approx \nu^2 V / \pi^2 c^3$  is the density of the radiation field modes (here  $V$  is effective volume of the gap,  $c$  is speed of light), and  $\langle \dots \rangle$  indicates averaging over the period of oscillation of the particle flux (eq 4).

Next we present numerical simulations for the model (eqs 1–3) using parameters taken from the experimental data of ref 18. In particular,  $T = 350$  K, excitation wavelength is  $\lambda_i = 532$  nm, and the vibrational frequency of the molecule is  $\omega_v \approx 2115$   $\text{cm}^{-1}$ . We also assume the effective volume of the gap to be  $V \approx 1 \times 5 \times 5 = 25$   $\text{\AA}^3$ , laser bandwidth is taken as  $\sim 1$  meV,<sup>39</sup> the amplitude of the bias oscillation in the junction  $|C_K| = 1.2$  eV,<sup>18</sup> and the coupling to the quantum field  $U_f \sim 0.01$  eV.<sup>40</sup> Note that  $U_f$  ( $M_v$ ) depends on the photon (vibration) frequency because of the usual term  $(\nu_f)^{1/2} ((\omega_v)^{1/2})$  in the bare coupling. The result is scaled by a factor of  $f = 10^{12}$ , which corresponds to the Raman enhancement observed in the experiment.<sup>18</sup> All scattering channel resonances are assumed to have the same

value  $\varepsilon_n = -1.75$  eV, which is estimated from the Hückel hopping matrix element value for silver together with an assumption that each metallic bridge between the nanoparticles consists of two Ag atoms. We choose Fermi energy as an origin,  $E_F = 0$ , and assume symmetric potential drop across the junction. (We assume that metallic bridges are equally well coupled to both nanospheres.) Electron-vibron coupling  $M_v$  is the only adjustable parameter. Fitting results of calculations to experimental data (see below) yields  $M_v \sim 0.1\omega_v$ , which is in the reasonable range. Calculations were performed on an energy grid spanning region from  $-20$  to  $20$  eV with step  $0.001$  eV.

Within our model, the slow time scale ( $T$ ) defines relative motion (fusion) of the two nanoparticles. Experimental data on Raman intensity suggest that spectra 1–19 correspond to nanoparticles approaching each other, with 19–37 measuring separation. For different spectra  $T \Gamma_n(T) = \Gamma_n \exp(-b|T - 19|)$ ,<sup>41</sup> where  $\Gamma_n = 342$   $\text{cm}^{-1}$  and  $b = 0.03$  are taken from the experimental line width. We assume all electron escape rates  $\Gamma_n$  to be equal, and the coupling to the two contacts is assumed to be symmetric  $\Gamma_{K,n} = \Gamma_n/2$  ( $K = L, R$ ).

Experimental observation of the Stark effect was discussed in the literature within chemical bonding and potential-induced frequency shift interpretations.<sup>42</sup> The former has its origin in CT between molecule and substrate, which leads to corresponding change in the molecular bond strength. The latter is caused by change of the effective molecular potential under local bias. Here we consider two metallic nanoparticles coupled by a metallic bridge. In this case local potential will be effectively screened. Thus below we assume the chemical bonding interpretation as the leading reason for the observed effect. Linear fit of the experimental data yields (see Figure 2a)



$$\Delta\omega_v(T) = 1.23 - |T - 19| \times \begin{cases} 0.05 & T \leq 19 \\ 0.07 & T > 19 \end{cases} \quad (8)$$

Here the shift is given in units of  $\text{cm}^{-1}$ .

Figure 2b compares experimental data for the CO-CTPR intensity with the results of the calculation. Assuming additive contribution to the Raman signal from scattering channels, eq 4, and utilizing the staircase observed in the intensity,<sup>18</sup> we estimate the number of scattering channels for each of the 37 spectra as shown in Figure 2c.

Several points are noteworthy: (1) The simple model (eqs 1–3) is capable of reproducing experimental data within the CTPR regime utilizing either experimental data or parameters from a reasonable range. (2) CT-SERS signal demonstrates staircase related to number of available channels for transport, which is similar to the behavior observed in electric current and thermal flux. (3) Exponential dependence of the CT-Raman signal on the interparticle distance is mostly related to the distance dependence of the electron tunneling matrix element.

To summarize, light scattering and electron transport are intimately related in current carrying junctions. We discussed theoretically one of possible mechanisms for the observed staircase in the CO-CTPR. Experimental data suggest possibility of formation (and destruction) of metallic bridges between the dumbbell nanoparticles during their fusion. Such bridges, assumed to be independent channels for conductance, yield quantized contributions to the CT Raman signal caused by tunneling electrons interaction with the CO vibration. We showed that for a simple model with parameters deduced from the experimental data, the measured Raman intensity staircase is fully compatible with the theoretical model of CT Raman scattering at a junction where the number of atomic contacts evolve slowly during the measurement process.

We note that we are considering a rather limited case of SERS; namely, Raman scattering when the junction plasmon is in the conductivity limit, which has not been previously addressed. The theoretical validation of the experimentally observed Raman staircase should be regarded as an important step in the exploration of this limit, which is dominated by quantum effects. We hope that newly developed methods that are designed to probe this limit, e.g., nanoparticle on mirror (NPOM)<sup>43</sup> and dual AFM junction configurations,<sup>44</sup> will critically test the offered theoretical framework and our experimental findings.

## ■ ASSOCIATED CONTENT

### ● Supporting Information

Derivation of eqs 4 and 5 for the model (eqs 1–3) is provided. This material is available free of charge via the Internet at <http://pubs.acs.org>.

## ■ AUTHOR INFORMATION

### Notes

The authors declare no competing financial interest.

## ■ ACKNOWLEDGMENTS

M.G. gratefully acknowledges support by the National Science Foundation (CHE-1057930) and the US-Israel Binational Science Foundation (Grant No. 2008282). This collaboration was made possible by the NSF Center for Chemical Innovation dedicated to Chemistry at the Space-Time Limit (CHE-082913).

## ■ REFERENCES

- (1) Jeanmaire, D. L.; Van Duyne, R. P. Surface Raman Spectroelectrochemistry: Part I. Heterocyclic, Aromatic, and Aliphatic Amines Adsorbed on the Anodized Silver Electrode. *J. Electroanal. Chem.* **1977**, *84*, 1–20.
- (2) Kneipp, K.; Moskovits, M.; Kneipp, H., Eds. *Surface-Enhanced Raman Scattering: Physics and Applications*; Springer: Heidelberg, Germany, 2010.
- (3) Gersten, J.; Nitzan, A. Electromagnetic Theory of Enhanced Raman Scattering by Molecules Adsorbed on Rough Surfaces. *J. Chem. Phys.* **1980**, *73*, 3023–3037.
- (4) Lombardi, J. R.; Birke, R. L.; Lu, T.; Xu, J. Charge-Transfer Theory of Surface Enhanced Raman Spectroscopy: Herzberg–Teller Contributions. *J. Chem. Phys.* **1986**, *84*, 4174–4180.
- (5) Nie, S.; Emory, S. R. Probing Single Molecules and Single Nanoparticles by Surface-Enhanced Raman Scattering. *Science* **1997**, *275*, 1102–1106.
- (6) Tian, J.-H.; Liu, B.; Li, X.; Yang, Z.-L.; Ren, B.; Wu, S.-T.; Tao, N.; Tian, Z.-Q. Study of Molecular Junctions with a Combined Surface-Enhanced Raman and Mechanically Controllable Break Junction Method. *J. Am. Chem. Soc.* **2006**, *128*, 14748–14749.
- (7) Ward, D. R.; Grady, N. K.; Levin, C. S.; Halas, N. J.; Wu, Y.; Nordlander, P.; Natelson, D. Electromigrated Nanoscale Gaps for Surface-Enhanced Raman Spectroscopy. *Nano Lett.* **2007**, *7*, 1396–1400.
- (8) Galperin, M.; Nitzan, A. Molecular Optoelectronics: The Interaction of Molecular Conduction Junctions with Light. *Phys. Chem. Chem. Phys.* **2012**, *14*, 9421–9438.
- (9) Masiello, D. J.; Schatz, G. C. Many-Body Theory of Surface-Enhanced Raman Scattering. *Phys. Rev. A* **2008**, *78*, 042505.
- (10) Jensen, L.; Aikens, C. M.; Schatz, G. C. Electronic Structure Methods for Studying Surface-Enhanced Raman Scattering. *Chem. Soc. Rev.* **2008**, *37*, 1061–1073.
- (11) Morton, S. M.; Jensen, L. Understanding the Molecule–Surface Chemical Coupling in SERS. *J. Am. Chem. Soc.* **2009**, *131*, 4090–4098.
- (12) Morton, S. M.; Silverstein, D. W.; Jensen, L. Theoretical Studies of Plasmonics Using Electronic Structure Methods. *Chem. Rev.* **2011**, *111*, 3962–3994.
- (13) Mullin, J. M.; Autschbach, J.; Schatz, G. C. Time-Dependent Density Functional Methods for Surface Enhanced Raman Scattering (SERS) Studies. *Comput. Theor. Chem.* **2012**, *987*, 32–41.
- (14) Galperin, M.; Ratner, M. A.; Nitzan, A. Raman Scattering from Nonequilibrium Molecular Conduction Junctions. *Nano Lett.* **2009**, *9*, 758–762.
- (15) Galperin, M.; Ratner, M. A.; Nitzan, A. Raman Scattering in Current-Carrying Molecular Junctions. *J. Chem. Phys.* **2009**, *130*, 144109.
- (16) Galperin, M.; Nitzan, A. Raman Scattering and Electronic Heating in Molecular Conduction Junctions. *J. Phys. Chem. Lett.* **2011**, *2*, 2110–2113.
- (17) Galperin, M.; Nitzan, A. Raman Scattering from Biased Molecular Conduction Junctions: The Electronic Background and Its Temperature. *Phys. Rev. B* **2011**, *84*, 195325.
- (18) Banik, M.; El-Khoury, P. Z.; Nag, A.; Rodriguez-Perez, A.; Guarrotxena, N.; Bazan, G. C.; Apkarian, V. A. Surface Enhanced Raman Trajectories on a Single Nano-Dumbbell: The Transition from Field to Charge Transfer Plasmons during the Fusion of the Spheres. *ACS Nano* **2012**, *6*, 10343–10354.
- (19) Ward, D. R.; Halas, N. J.; Cizek, J. W.; Tour, J. M.; Wu, Y.; Nordlander, P.; Natelson, D. Simultaneous Measurements of Electronic Conduction and Raman Response in Molecular Junctions. *Nano Lett.* **2008**, *8*, 919–924.
- (20) Guarrotxena, N.; Ren, Y.; Mikhailovsky, A. Raman Response of Dithiolated Nanoparticle Linkers. *Langmuir* **2011**, *27*, 347–351.
- (21) Banik, M.; Nag, A.; El-Khoury, P. Z.; Perez, A. R.; Guarrotxena, N.; Bazan, G. C.; Apkarian, V. A. Surface-Enhanced Raman Scattering of a Single Nanodumbbell. *J. Phys. Chem. C* **2012**, *116*, 10415–10423.

- (22) Esteban, R.; Borisov, A. G.; Nordlander, P.; Aizpurua, J. Bridging Quantum and Classical Plasmonics with a Quantum-Corrected Model. *Nat. Commun.* **2012**, *3*, 825.
- (23) Romero, I.; Aizpurua, J.; Bryant, G. W.; Abajo, F. J. G. D. Plasmons in Nearly Touching Metallic Nanoparticles: Singular Response in the Limit of Touching Dimers. *Opt. Express* **2006**, *14*, 9988–9999.
- (24) Lassiter, J. B.; Aizpurua, J.; Hernandez, L. I.; Brandl, D. W.; Romero, I.; Lal, S.; Hafner, J. H.; Nordlander, P.; Halas, N. J. Close Encounters between Two Nanoshells. *Nano Lett.* **2008**, *8*, 1212–1218.
- (25) Perez-Gonzalez, O.; Zabala, N.; Aizpurua, J. Optical Characterization of Charge Transfer and Bonding Dimer Plasmons in Linked Interparticle Gaps. *New J. Phys.* **2011**, *13*, 083013.
- (26) Marinica, D.; Kazansky, A.; Nordlander, P.; Aizpurua, J.; Borisov, A. G. Quantum Plasmonics: Nonlinear Effects in the Field Enhancement of a Plasmonic Nanoparticle Dimer. *Nano Lett.* **2012**, *12*, 1333–1339.
- (27) Esteban, R.; Borisov, A. G.; Nordlander, P.; Aizpurua, J. Bridging Quantum and Classical Plasmonics with a Quantum-Corrected Model. *Nat. Commun.* **2012**, *3*, 825.
- (28) Xu, B.; Tao, N. J. Measurement of Single-Molecule Resistance by Repeated Formation of Molecular Junctions. *Science* **2003**, *301*, 1221–1223.
- (29) Schwab, K.; Henriksen, E. A.; Worlock, J. M.; Roukes, M. L. Measurement of the Quantum of Thermal Conductance. *Nature* **2000**, *404*, 974–977.
- (30) Li, G.; Shishodia, M. S.; Fainberg, B. D.; Apter, B.; Oren, M.; Nitzan, A.; Ratner, M. A. Compensation of Coulomb Blocking and Energy Transfer in the Current Voltage Characteristic of Molecular Conduction Junctions. *Nano Lett.* **2012**, *12*, 2228–2232.
- (31) Park, T.-H.; Galperin, M. Correlation between Raman Scattering and Conductance in a Molecular Junction. *Europhys. Lett.* **2011**, *95*, 27001.
- (32) Park, T.-H.; Galperin, M. Charge Transfer Contribution to Surface-Enhanced Raman Scattering in a Molecular Junction: Time-Dependent Correlations. *Phys. Rev. B* **2011**, *84*, 075447.
- (33) Galperin, M.; Nitzan, A. Optical Properties of Current Carrying Molecular Wires. *J. Chem. Phys.* **2006**, *124*, 234709.
- (34) Mukamel, S. *Principles of Nonlinear Optical Spectroscopy*; Oxford Series in Optical and Imaging Sciences; Oxford University Press: New York, 1995; Vol. 6.
- (35) Persson, B. N. J. On the Theory of Surface-Enhanced Raman Scattering. *Chem. Phys. Lett.* **1981**, *82*, 561–565.
- (36) Oren, M.; Galperin, M.; Nitzan, A. Raman Scattering from Molecular Conduction Junctions: Charge Transfer Mechanism. *Phys. Rev. B* **2012**, *85*, 115435.
- (37) Jauho, A.-P.; Wingreen, N. S.; Meir, Y. Time-Dependent Transport in Interacting and Noninteracting Resonant-Tunneling Systems. *Phys. Rev. B* **1994**, *50*, 5528–5544.
- (38) Mahan, G. D. *Many-Particle Physics*; Plenum Press: New York, 1990.
- (39) White, A. J.; Fainberg, B. D.; Galperin, M. Collective Plasmon-Molecule Excitations in Nanojunctions: Quantum Consideration. *J. Phys. Chem. Lett.* **2012**, *3*, 2738–2743.
- (40) Sukharev, M.; Galperin, M. Transport and Optical Response of Molecular Junctions Driven by Surface Plasmon Polaritons. *Phys. Rev. B* **2010**, *81*, 165307.
- (41) Galperin, M.; Nitzan, A.; Ratner, M. A. Molecular Transport Junctions: Current from Electronic Excitations in the Leads. *Phys. Rev. Lett.* **2006**, *96*, 166803.
- (42) Lambert, D. K. Vibrational Stark Effect of Adsorbates at Electrochemical Interfaces. *Electrochim. Acta* **1996**, *41*, 623–630.
- (43) Mubeen, S.; Zhang, S.; Kim, N.; Lee, S.; Kramer, S.; Xu, H.; Moskovits, M. Plasmonic Properties of Gold Nanoparticles Separated from a Gold Mirror by an Ultrathin Oxide. *Nano Lett.* **2012**, *12*, 2088–2094.
- (44) Savage, K. J.; Hawkeye, M. M.; Esteban, R.; Borisov, A. G.; Aizpurua, J.; Baumberg, J. J. Revealing the Quantum Regime in Tunnelling Plasmonics. *Nature* **2012**, *491*, 574–577.